

ULTRA-HIGH BRIGHTNESS ELECTRON BEAMS BY ALL OPTICAL PLASMA BASED INJECTORS

V. Petrillo, Università degli Studi, Milano (Italy)

L. Serafini, P. Tomassini, INFN, Milano (Italy)

C. Benedetti, P. Londrillo, A. Sgattoni, G. Turchetti Università e INFN Bologna (Italy)

Abstract

We studied the generation of low emittance high current mono-energetic beams from plasma waves driven by ultra-short laser pulses, in view of achieving beam brightness of interest for FEL applications. We have studied a regime based on a LWFA plasma driving scheme on a gas jet modulated in areas of different densities with sharp density gradients. Simulations carried out using VORPAL show that, using a properly density modulated gas jet, it is possible to generate beams at energies of about 30 MeV with peak currents of 20 kA, slice transverse emittances as low as $0.3 \mu\text{m}$ and energy spread around 0.4 %. These beams break the barrier of $10^{18} \text{ A}/(\text{mm.mrad})^2$ in brightness, opening a new range of opportunities for FEL applications. An example of Free Electron Lasers driven by such kind of beams injected into laser undulators is shown. The system constituted by the electron beam under the effect of the e.m. undulator has been named AOFEL (for All Optical Free-Electron Laser).

INTRODUCTION

Recently a few authors proposed to use plasma injectors as electron beam driver for SASE X-ray Free-Electron Lasers: the aim is to design compact and powerful Free Electron Lasers. Gruner et al. [1] proposed to operated in the bubble regime to generate an electron beam with very high brightness at 1 GeV, with a beam peak current of 100 kA and rather good normalized emittance (1 mm.mrad) and low energy spread (0.1 %) and to inject the beam in a magnetic undulator.

In this paper we present a different approach, which has in common the goal to use a plasma injector to drive a compact SASE FEL, but differing in the regime used in the plasma channel to generate the beam and in the energy of the electrons, which is in the range of a few tens of MeV. To this purpose the use of an electromagnetic undulator, i.e. a counter propagating laser pulse of proper wavelength, is foreseen, as recently proposed [2]. The technique of controlling the breaking of the plasma wave by tapering the plasma density in the gas-jet is applied, as proposed in [3]: we believe this technique is suitable to produce high quality beams than the bubble regime, though with lower beam currents (tens of kA instead of higher than 100 kA). In addition, the use of a e.m. undulator allows to conceive an ultra-compact device, characterized by a few mm of total length.

E-BEAM GENERATION VIA LWFA

Laser wakefield acceleration (LWFA) of e-beams [4] has been proved to be able to produce high energetic (up

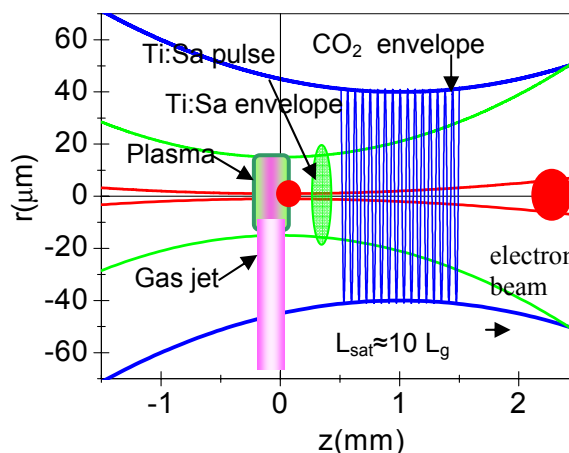


Figure 1: Lay-out of the experiment for the case of the CO₂ electromagnetic undulator for which the plasma density is over critical (see text for details).

to the GeV scale) quasi-monochromatic electron beams by using ultra-short (tens of femtosecond long) laser pulses and a plasma as accelerating medium. In LWFA the longitudinal ponderomotive force of the laser pulse excites a plasma wave whose longitudinal (i.e. accelerating) electric field can exceeds thousands times that of RF-guns. A critical issue for achieving high-quality e-beams is represented by a good control in particle injection into the plasma wave, whose phase speed equals the group velocity of the laser pulse.

In this paper we will show results of numerical simulation in the nonlinear LWFA regime with longitudinal injection after density downramp. In this scheme the electrons of the crest of the waves are longitudinally injected in the fast running wakefield by a partial break of the wave induced by a sudden change in its phase speed at the transition. If the laser pulse waist w_0 is much larger than the wave wavelength $\lambda_p \cong \sqrt{1.1 \cdot 10^{21} / n_e^2}$, n_e being the plasma electron density in cm^{-3} , the transverse dynamics is negligible at the transition and an electron bunch with an extremely low

transverse emittance is created and injected in the acceleration region of the wave .

We searched for parameters giving rise to electron bunches suitable for driving the laser-based FEL source, i.e., for bunches that must have a high current but don't need to have overall low emittance and energy spread. They should contain slices with very low slice emittance and very low slice energy spread, instead.

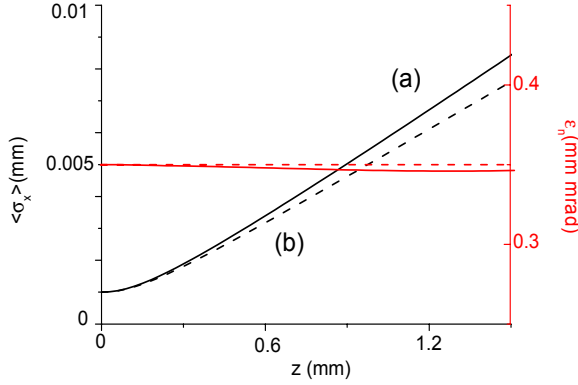


Figure 2: Envelope $\langle \sigma_x \rangle$ and transverse normalized emittance ϵ_n versus z as given by Astra in vacuum for a typical AOFEL beam with $I=20$ kA, $\epsilon_n(z=0)=0.3$ mm mrad, $\langle \sigma_x \rangle(z=0)=1\mu\text{m}$ and $\gamma=60$.

We expect space charge effects to occur over a beam-plasma wavelength scale, which is given by $\lambda_{L,sp} = 2\pi\gamma R \sqrt{\frac{2\gamma I_0}{In}}$, R being the beam radius, I its current, γ the mean Lorentz factor of the electrons and $I_0 = 17$ kA the Alfvén current. For our typical beam this length is of the order of a cm, much longer than the expected saturation length in the e.m. undulator (which is of the order of 1 mm or a fraction of it). This implies that we should not expect serious emittance degradation due to transverse space charge along the e.m. undulator, as can be seen from Figure 2, which presents a simulation made with ASTRA for a typical All Optical Free-Electron Laser (AOFEL) beam initially focussed to $1\mu\text{m}$ rms spot size and then freely propagating in a 1.5 mm long drift. The rms beam envelope $\langle \sigma_x \rangle$ (left scale) and the rms normalized emittance ϵ_n (right scale) are shown on the range of interest along the coordinate z , both with (curves (a)) and without (curves (b)) the effects of the space charge for $I=20$ kA, $\epsilon_n=0.3$ μm and $\gamma=60$. The predicted gain length is about $50\mu\text{m}$, so that the beam evolution is followed for about 30 gain lengths. In 1.5 mm of drift the emittance does not change significantly, while the envelope evolves as if the space charge is absent.

Clearly, there may be effects of energy spread increase due to longitudinal and transverse space charge fields, including retarded effects at plasma-vacuum interface.

Simulations were performed with the fully self-consistent Particle-In-Cell (PIC) code VORPAL [5] in the 2.5D (3D in the fields, 2D in the coordinates) configuration.

X-ray FELs

The initial plasma density profile (see Fig. 3) is composed by a smooth rising edge (laser coming from the left) and a first plateau of density n_{01} , with appropriate phase of the plasma wave excited in the second plateau (accelerating region). Simulations of the injection-acceleration process were performed in a moving window of longitudinal and transverse size of $50\mu\text{m}$ and $60\mu\text{m}$, respectively, sampled in an 800×120 box with 20 macroparticles/cell, corresponding to a longitudinal and transverse resolutions of $\lambda_0/14$ and $\lambda_0/2$, respectively.

In Figure 4 some snapshots of the electron density are reported. In Fig 4 (a) the laser pulse (coming to the left hand side) is crossing the transition and the plasma wave in the first plateau is experiencing nonlinear steepening. In Fig 4 (b) the laser pulse is well inside the second plateau (the accelerating region) and the second crest of the plasma wave has partially broken.

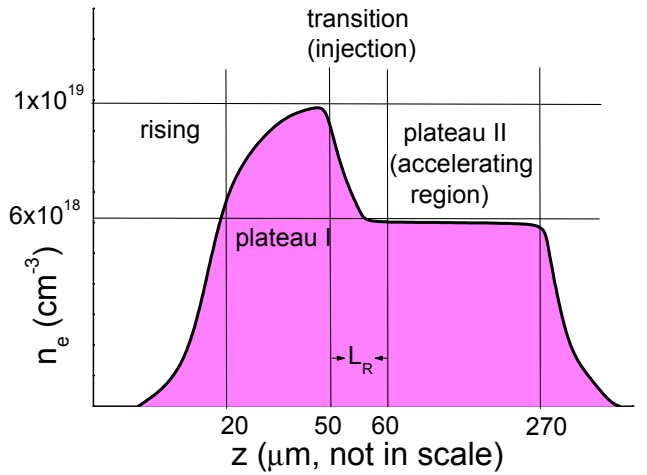


Figure 3: Background plasma density n_e versus z useful for e-beam injection and acceleration

The electrons injected in the wave are suddenly accelerated and focused by the longitudinal and transverse forces of the wakefield (Fig 4 (c)). After an acceleration length of about $200\mu\text{m}$ the electron beam is still focused (Fig 4 (d)) and gets a maximum energy of about 28MeV. The final parameters of the initial plasma density have been obtained by an optimization procedure in the parameters double-plateau profile, i.e. the second plateau density, the transition scale-length and the amplitude of the transition. The first parameter controls the plasma wavelength and maximum accelerating gradient in the acceleration region and must be tuned according to the e-beam length and charge. The transition scale-length controls the charge and length of the beam and must be as small as possible in order to ensure the trapping of the largest number of particles, while a tuning in the amplitude of the transition is necessary for selecting the appropriate phase of the particles in the Langmuir wave.

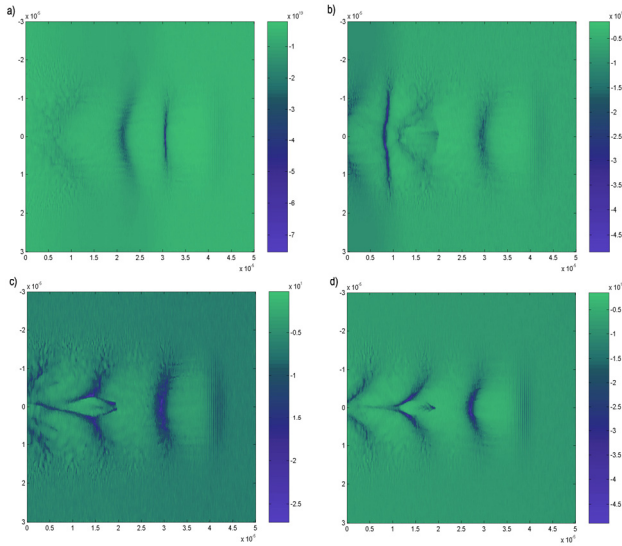


Figure 4: Snapshot of the electronic density when the laser pulse is in the first plateau (a), the laser pulse is crossing the transition (b), the laser pulse is just in the accelerating region (c) and the laser pulse has propagated for about 200 μm in the accelerating region (d).

The parameters of the plasma are reported in Table 1 together with the parameters of the laser.

Table 1: Plasma and Laser Parameter

Energy (J)	2
Waist (μm)	20
Intensity (W/cm^2)	$7 \cdot 10^{18}$
Duration (fs)	20
n_{01} (cm^{-3})	$1 \cdot 10^{19}$
L_R (μm)	10
n_{02} (cm^{-3})	$0.6 \cdot 10^{19}$
λ_p (μm)	13

FEL SIMULATIONS

The electron bunch produced by VORPAL has been analysed for finding the slices characterized by the highest brightness for producing FEL radiation [5]. Fig 5 shows the longitudinal phase space. The part shaded, delimited by $z=1.1 \mu\text{m}$ and $1.59 \mu\text{m}$, satisfies both conditions of large current and low energy spread and is suitable for producing FEL radiation. The average values for this part of the bunch are: $\gamma=55.2$, $I=20 \text{ kA}$, $\langle\sigma_x\rangle=0.5\mu\text{m}$, $\delta\gamma/\gamma=1.2 \cdot 10^{-2}$ and $\epsilon_n=0.3 \mu\text{m}$. We suppose to let the beam defocus up to $\langle\sigma_x\rangle=5\mu\text{m}$ and subject it to the field of a CO_2 laser with wavelength $\lambda_L=10 \mu\text{m}$ and intensity $a_L=0.8$.

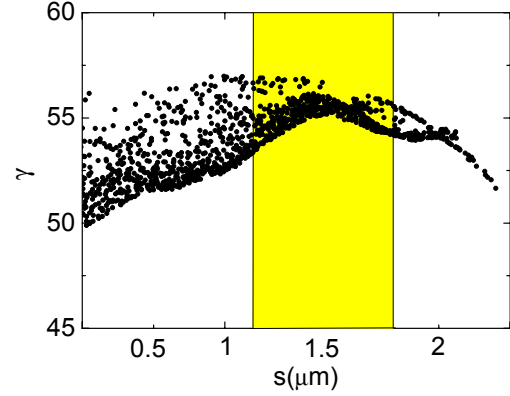


Figure 5: the longitudinal phase space γ vs s . In yellow the part of phase space that contributes to the emission.

For these values the radiation wavelength is $\lambda_R=1.35 \text{ nm}$, the FEL parameter $\rho=310^{-3}$, the cooperation length $L_c = \frac{\lambda_R}{4\pi\sqrt{3}\rho} = 0.14 \mu\text{m}$.

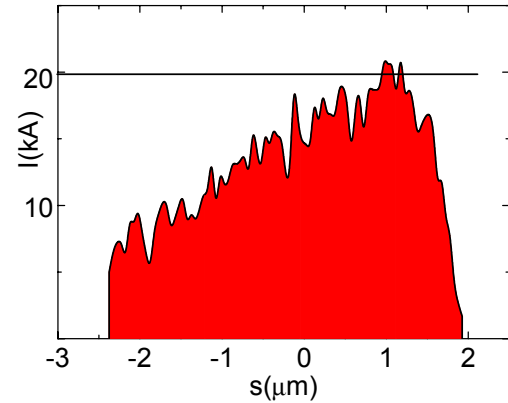


Figure 6: Current profile (kA) vs s .

In this case, $L_b/(2\pi L_c)=0.566$ and the condition $L_b/2\pi L_c < 1$ for a clean single spike production turns out to be satisfied.

The laser beam interaction has been simulated with the code GENESIS 1.3 [7], which tracks the particles in a static wiggler. By exploiting the equivalence between static and electromagnetic undulators [3], we have imported the particle of the radiating slice into GENESIS 1.3, obtaining the results presented in Fig 6. Window (a) shows the average power P vs the coordinate along the undulator z , while window (b) presents the peak power vs z . In fig 6 (c) there is the shape of the power vs s and in (d) the spectrum of the X-rays pulse at $z=2.5\text{mm}$. The peak power value is 0.2 GW, the total energy 0.12 μJ and the structure of the power on the beam is that typical of superradiance.

The main properties of the radiation are summarized in Table 2 for the first peak occurring after 1 mm of

propagation in the electromagnetic field of the laser and at saturation, taking place at 5 mm. Here, P_{\max} is the maximum power emitted, E is the average energy yield, L_R is the radiation pulse width, L_{sat} is the saturation length, and $d\lambda_R/\lambda_R$ is the bandwidth.

In this paper we propose the possibility of using a LWFA plasma driving scheme on a gas jet modulated in areas of different densities with sharp density gradients to generate a mono-energetic, high current (> 20 kA) electron beam.

This bunch of electrons, characterized by the presence of low emittance (<0.5 mm mrad), low energy spread slices, when interacting with a counter propagating CO₂ laser pulse, radiates a single spike, highly coherent, ultrashort (< 1 fsec) X-ray pulse via excitation of a SASE superradiant FEL instability. The peak power achieved at 1.2 nm is of the order of 200 MW.

Taking an electromagnetic undulator at 1 μm wavelength the electron beam can drive a 1 Ang FEL, with similar performances.

Although the presented analysis is based on three-dimensional simulations, effects due to alignment errors, spatial and temporal jitters, as well as realistic laser pulse profiles for the e.m. undulator and consistent exit from the plasma, that have not been yet considered, must be thoroughly investigated in order to assess the experimental feasibility of such a new FEL scheme.

Table 2: Main Characteristics of the Radiation

	First peak	Saturation
P_{\max} (W)	$2 \cdot 10^8$	$1.5 \cdot 10^8$
E (μJ)	0.05	0.12
L_R (μm)	0.05	0.5
L_{sat} (μm)	1.	4.5
λ_R (nm)	1.35	
$d\lambda_R/\lambda_R$	0.81%	

Nevertheless, we believe that our analysis, although very preliminary and missing a full self-consistent start-to-end simulation, shows a potential for the future development of an ultra-compact source of coherent X rays at brilliance levels comparable to those typical of fourth generation light sources. Further work is in progress with more consistent simulations able to describe the exit of the beam from the plasma and the transport through the e.m. undulator, in order to address the problem of performing a real start-to-end simulation from the plasma to the FEL radiation production.

REFERENCES

[1] F. Grüner, et al: Appl. Phys. B 86, 431-435 (2007)
 [2] A. Bacci et al: P. R. ST AB 9, 060704 (2006)
 [3] S. Bulanov et al: Phys. Rev. E 58 R5257 (1998)
 [4] P. Tomassini: Phys. Rev. ST-AB 6, 121301 (2003)
 [5] C. Nieter and J. R. Cary: Journal of Computational Physics, Volume 196, Issue 2, p. 448-472 (20 May 2004).
 [6] V. Petrillo, L. Serafini, P. Tomassini: PRSTAB 11, 070703 (2008)
 [7] S. Reiche: Nucl. Instrum. Methods Phys. Res. A 429, 243 (1999)

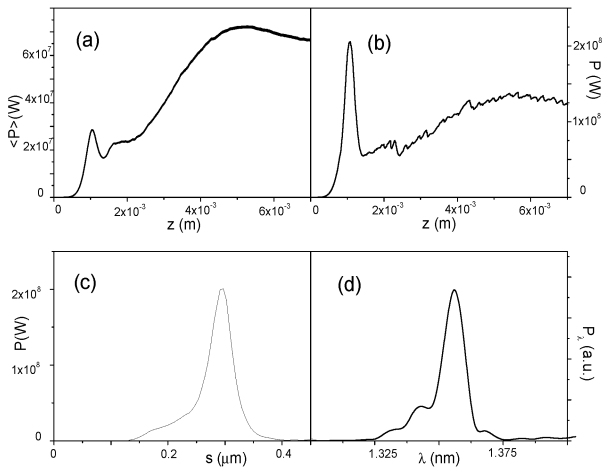


Figure 10: (a) average power P (W) vs the coordinate along the undulator z (m); (b) peak power along z ; (c) power profile along the bunch coordinate s (μm) at $z=2.5$ mm; (d) power spectrum at $z=2.5$ mm.